Electronic Supplementary Material (ESI) for Nanoscale.

Supplementary Information

A Transparent Flexible Z-Axis Sensitive Multi-Touch Panel Based on Colloidal ITO Nanocrystals

Neralagatta M. Sangeetha, Mélanie Gauvin, Nicolas Decorde, Fabien Delpech, Pier F. Fazzini, Benoit Viallet, Jérémie Grisolia, Guillaume Viau and Laurence Ressier*

Université de Toulouse, LPCNO, INSA-CNRS-UPS, 135 Avenue de Rangueil, Toulouse 31077, France

* Corresponding author: E-mail: laurence.ressier@insa-toulouse.fr

1. Morphological characterization of ITO nanocrystals (NCs) synthesized under different experimental conditions, by transmission electron microscopy (TEM)

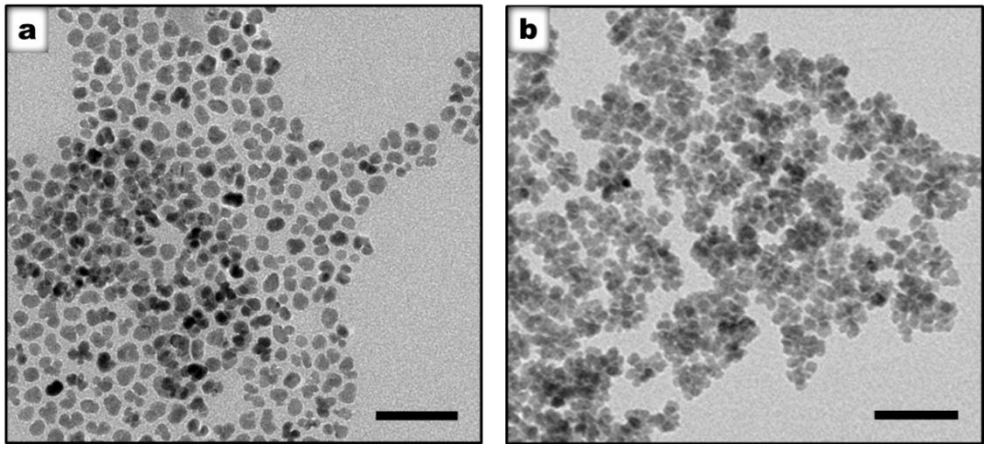

Figure S1. TEM images of ITO nanocrystals synthesized by auto-decomposition of (a) the In/Sn oleates (1:3 of In+Sn to oleic acid) and (b) the In/Sn octanoates (1:4 In+Sn to octanoic acid) at 290 °C. The NC morphology is different from that prepared by oleylamine injection at 290 °C, which yield spherical nanocrystals. Scale bars = 50 nm.

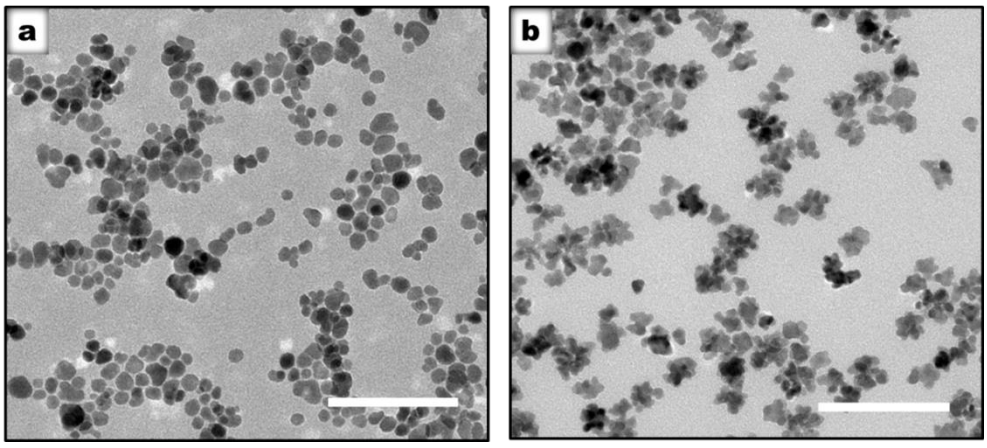

Figure S2. TEM images of ITO nanocrystals synthesized by mixing the In/Sn acetate precursors with both (a) octanoic acid and oleylamine, (b) butanoic acid and oleylamine in the beginning of the reaction and decomposed at 290 °C. Scale bars = 100 nm.

2. Crystallographic structure and chemical composition of the ITO NCs by X-ray diffraction (XRD), high-resolution transmission electron microscopy (HRTEM) and scanning TEM based on energy dispersive X-ray (STEM-EDX) imaging

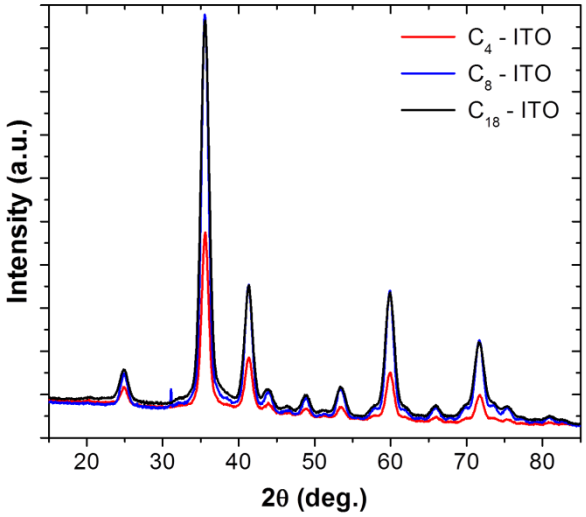

Figure S3. Typical powder XRD patterns of the oleate (black), octanoate (blue) and butanoate (red) ITO nanocrystals.

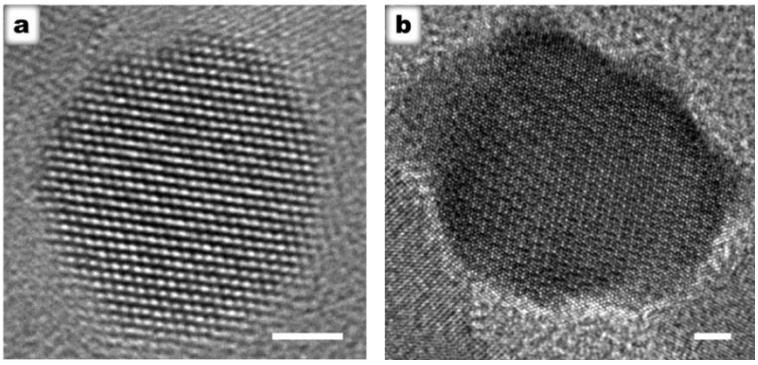

Figure S4. Representative HRTEM images of (a) octanoate and (b) butanoate ITO nanocrystals. Scale bars = 2 nm.

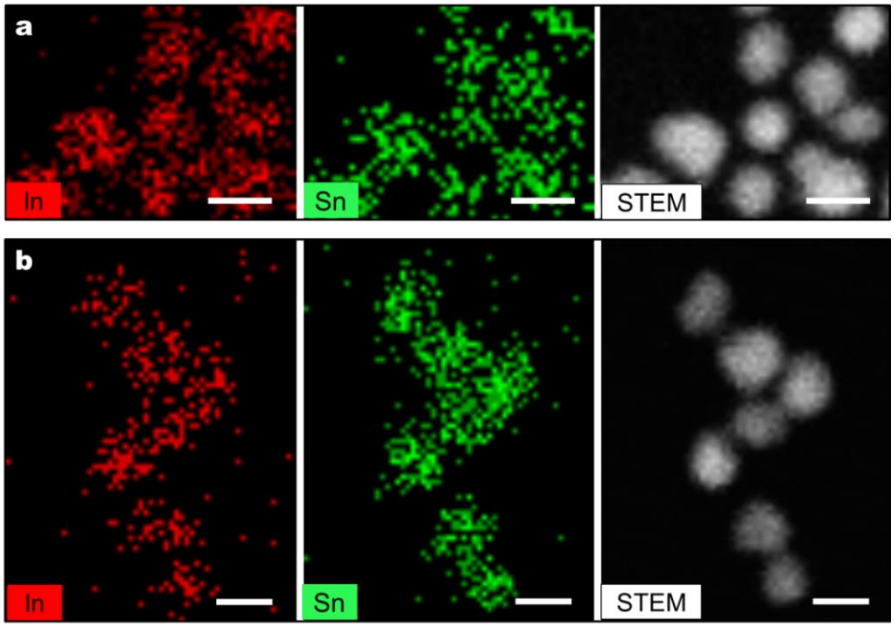

Figure S5. STEM-EDX elemental mappings of (a) octanoate and (b) butanoate stabilized ITO nanocrystals: indium map (left), tin map (center) and the corresponding overlay (right). Scale bars = 8 nm.

3. Characterization of the surface protecting layer of the ITO NCs by Fourier transform infra-red (FT-IR) spectroscopy and nuclear magnetic resonance (NMR) spectroscopy

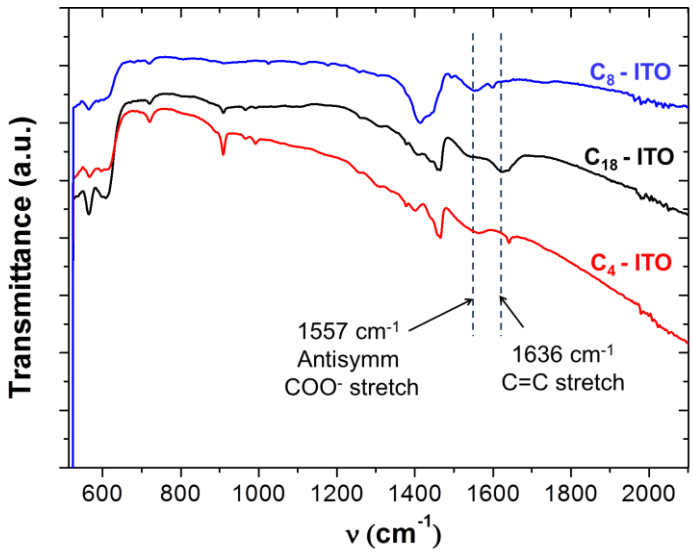

Figure S6. FT-IR of the oleate (black), octanoate (blue) and butanoate (red) stabilized ITO nanocrystals. The presence of carboxylate group is indicated by the broad signal at 1557 cm^{-1}. Noteworthy is the absence of the C=C stretching signal at 1636 cm^{-1}, in the octanoate ITO NC sample. A sharp signal around this frequency for butanoate ITO NC sample suggests the presence of free oleylamine.

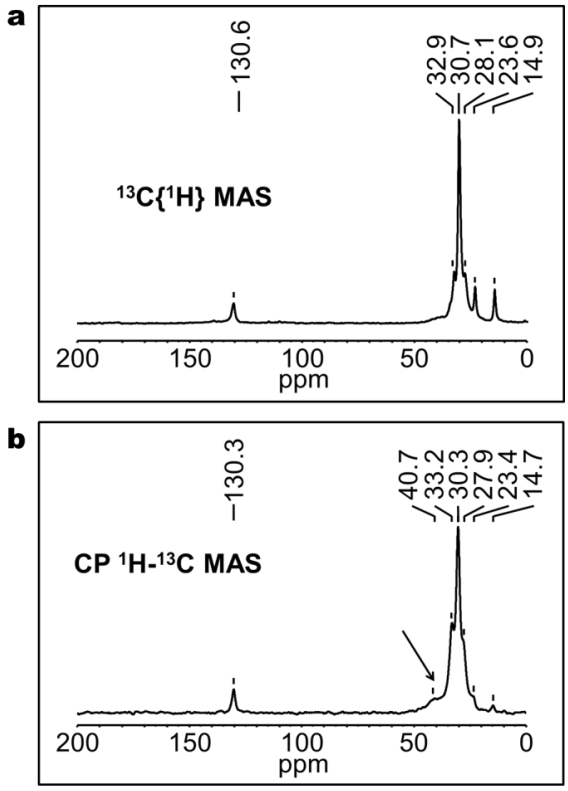

Figure S7. (a) $^{13}C\{^{1}H\}$ MAS NMR spectrum and (b) cross-polarization ^{1}H-^{13}C MAS NMR spectrum of the oleate ITO NCs (the arrow points to the α-CH_2 of oleylamine).

Table S1. Diffusion coefficients of the ligand mixtures in $CDCl_3$ measured by DOSY-NMR and corresponding hydrodynamic diameters calculated using the Stokes-Einstein relationship.

Ligand	**Diffusion coefficient *D* ($m^2.s^{-1}$)**	**Hydrodynamic diameter *d* (nm)**
Oleic acid/Oleyl amine 0.095/0.122 mmoles	6×10^{-10} 4×10^{-10}	0.66 1.00
Octanoic acid/Oleyl amine 0.104/0.122 mmoles	6×10^{-10} 3.9×10^{-10}	0.66 1.02
Butanoic acid/Oleyl amine 0.135/0.122 mmoles	3.9×10^{-10}	1.02

4. Structural characterization of ITO NC films deposited by CSA on flexible PET substrates, by scanning electron microscopy (SEM)

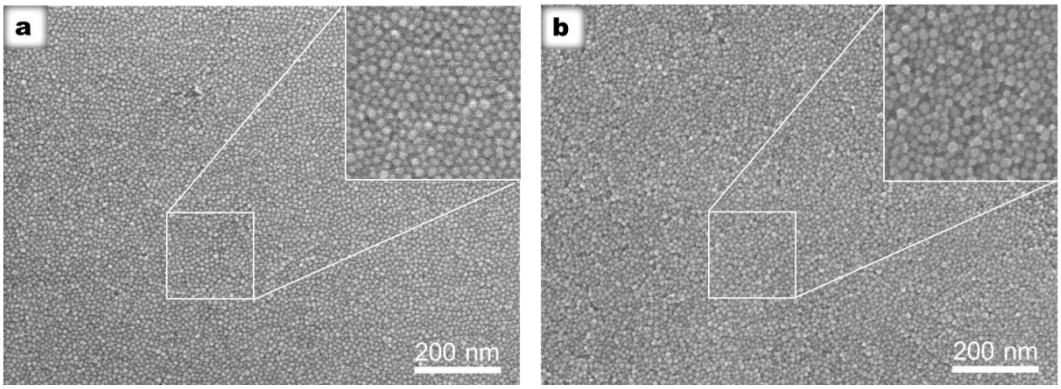

Figure S8. Wide-area SEM images of (a) a 120 nm thick film of oleate ITO NCs, and (b) a 130 nm thick film of octanoate ITO NCs on PET substrates fabricated by CSA. The zoomed-in images in the inset show the close-packed NC arrangement within the films in both cases.

5. Electrical characterization of ITO NC films at room temperature: resistance and resistivity

The electrical measurements performed on oleate, octanoate and butanoate ITO NC-based films show linear current-voltage characteristics at room temperature. As an example, Figure S9 presents typical current-voltage characteristics for a 160 nm thick butanoate ITO NC film measured between +/-3 V. Because of this linearity (Ohmic behavior), we could define the resistance R_0 taken at T= 300 K to characterize each ITO NC film.

Interestingly, despite the lack of long range ordering of NCs within the films, doubling the gap between the electrodes (*ie* doubling the length of the NC film) leads to a doubling of the film resistance. As shown in Figure S9, R_0 ~9 MΩ for a gap of 50 µm and R_0~18 MΩ for a gap of 100 µm in the case of a 160 nm butanoate ITO NC film. This proportionality allowed us to introduce resistivity as a relevant physical parameter to describe the electrical characteristics of the NC films. The resistivity of the ITO NC films ρ_0 at room temperature was calculated using the relation:

$$\rho_0 = \frac{W.H}{L} R_0$$

where W, H and L are the width, the thickness and the length, respectively of the NC film connected between the electrodes.

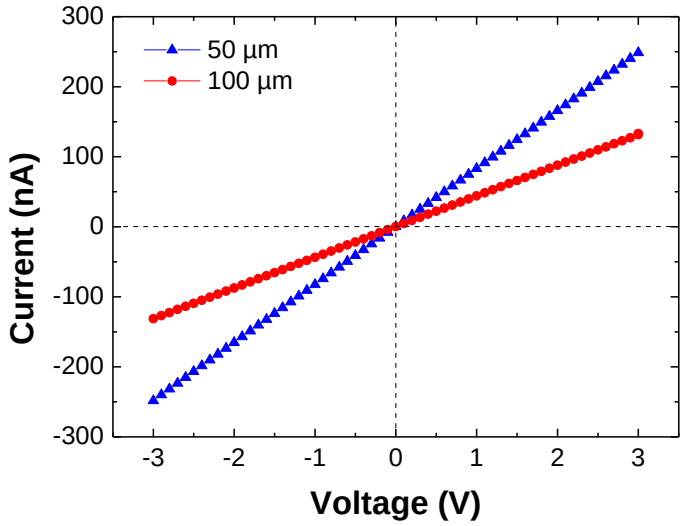

Figure S9. Typical current-voltage characteristics at 300 K of a 160 nm thick film of butanoate ITO NCs connected between two electrodes separated by gaps of 50 µm (blue triangle symbols) and 100 µm (red disk symbols).